DOI: 10.1002/ejic.200701116

Synthesis, Structures and Ion-Association Properties of a Series of Schiff Base Oxidovanadium(V) Complexes with 4-Substituted Long Alkoxy Chains

Yuriko Abe,*[a] Ayako Iyoda,[a] Kanako Seto,[a] Ayano Moriguchi,[a] Tomoaki Tanase,[a] and Haruhiko Yokoyama[b]

Keywords: Schiff base ligands / Oxidovanadium(V) complexes / Crystal-to-crystal transformation / Ion association / DFT calculations

Schiff base VO_2^V and VO^V complexes with long 4-substituted alkoxy chains have been synthesised from the corresponding VO^{IV} complexes, [VO{(4-$C_nH_{2n+1}O)_x$salen}] [x = 1, 2, *n* = 3–16 and salen = *N*,*N*′-ethylenebis(salicylideneiminato)], in solutions in the absence or presence of $HClO_4$ under aerobic conditions. The green single-crystals of the VO^{IV} complexes (x = 2, *n* = 3, 4, 6) coexisting with solutions without $HClO_4$ turned slowly to the yellow single-crystals of the species with *n* = 3 (**1**) and 4 (**2**), a process which took several months. An X-ray crystallographic analysis revealed that the VO^{IV} complexes are transformed into the dimeric VO_2^V complexes with the tridentate sal-en (sal-en = *N*-salicylideneethylenediamine) ligand from the tetradentate salen moieties. However, the single crystals of the VO^{IV} complexes with longer alkoxy chains of $n \geq 8$ did not yield the corresponding yellow crystals of the VO_2^V complexes. This crystal-to-crystal transformation is discussed in relation to the crystal packing structures of the VO^{IV} complexes. In contrast, addition of $HClO_4$ solution to two series with one and two alkoxy chains in the 4-positions immediately afforded the corresponding blue VO^V perchlorate complexes, [VO{(4-$C_nH_{2n+1}O)_x$salen}]-ClO_4 (x = 1, 2) without transformation of the salen moieties. The structure of **8**·MeOH·0.5H_2O determined from an X-ray crystallographic analysis was a unique dimeric structure supported by electrostatic stacking and CH–π interactions in an octahedral environment. The DFT calculations were studied to obtain the stabilisation energy for the dimerisation. Furthermore, in methanol solution, the effects of the alkoxy chain lengths on the ion association were investigated by conductivity measurements. The ion-association state in methanol solution is discussed with the solid-state structure.

Introduction

Vanadium complexes have been a growing topic of investigation because of their versatile physico-chemical properties, bioactivities and catalytic properties in organic and inorganic transformations.[1–3] With regards to the physico-chemical properties, the liquid crystals with transition-metal core groups such as VO^{IV} and Pt^{II}, known as metallomesogens, are a fascinating branch of nanostructural materials because the self-assemblies of coordinated metal complexes enhance the physico-chemical properties with new functionalities thereby increasing their potential range of applications.[4–5] Schiff base ligands provide a wide range of ways for modifying liquid crystal compounds so that the possibility and nature of mesomorphic properties have been investigated.[6–8] The chemistry of VO^{IV} and VO^V Schiff base complexes with square pyramidal structures that do not have long alkoxy or alkyl chains has been extensively studied[9–11] and has been shown to be dominated by the stable oxidovanadium (V=O) groups which retain their functions and are responsible for their unique structures.[12] For the VO^{IV} salen [salen = *N*,*N*′-ethylenebis(salicylideneiminato)] complexes containing Schiff base ligands with two long alkoxy chains at the 5-positions on aromatic rings, the occurrence of the liquid crystalline phase of the smectic A (S_A) or C (S_C) phase has been reported at higher temperatures.[8d] However, the VO^{IV} 5-alkoxysalpn complexes [salpn = *N*,*N*′-propylenebis(salicylideneiminato)] do not exhibit liquid crystallinity because of the strong interactions through the linear V=O chains. To date, there has been no systematic investigation concerning the molecular assemblies and metallomesogens of VO^{IV} salen and salpn complexes with two long alkoxy chains at the 4-positions compared with those with 5-substituted derivatives.[8d,8e] We recently reported the syntheses, crystal structures and liquid properties of a series of matal-salen and -salpn complexes containing 4-substituted alkoxy chains of aromatic rings, [M{(4-$C_nH_{2n+1}O)_2$salen}] (M = VO^{IV},[13a] Ni^{II},[13b] Cu^{II},[13c] *n* = 3–20) and [VO{(4-$C_nH_{2n+1}O)_2$salpn}] (*n* = 8–18).[13a] The

[a] Department of Chemistry, Faculty of Science, Nara Women's University,
Kitauoya-nishimachi, Nara 630-8506, Japan
E-mail: yabe@cc.nara-wu.ac.jp
[b] International Graduate School of Arts and Sciences, Yokohama City University,
Seto, Kanazawa-ku, Yokohama 236-0027, Japan
E-mail: yokoyama@yokohama-cu.ac.jp

VO^{IV} complexes with n = 16–20 transfer from the bilayer crystal to the novel bilayer metallomesogens [M($Pa2_1$) mesophase]. On the other hand, the 4-alkoxysalpn complexes show the unusual rectangular columnar mesophase (Col_r) with the linear chain via the V=O units. The mesomorphic properties of metallomesogens can be remarkably varied by the selection of the metal ion and the positions of the substituents on the aromatic rings of the salen moieties.

In this study we describe the synthesis, structures and ion-association properties of a series of Schiff base oxidovanadium(V) complexes with long 4-substituted alkoxy chains. In particular, to date, there have been few reports on the structures and characteristics of VO_2^V and VO^V complexes with long alkoxy chains. We have found that the green single-crystals of the VO^{IV} complexes, [VO{(4-$C_nH_{2n+1}O)_2$salen}] (n = 3, 4, and 6) turn slowly to the yellow single-crystals of the VO_2^V complexes in solutions over several months under aerobic conditions but when crystals of the VO^{IV} complexes were completely dissolved, the resultant green solutions did not change into the yellow solutions. The crystal structures of the VO_2^V complexes of n = 3 (**1**) and 4 (**2**) have been determined by X-ray crystallographic analyses. Interestingly, the VO^{IV} complexes with alkoxy chains longer than n = 8 did not turn to the corresponding yellow single-crystals of the VO_2^V complexes. This crystal-to-crystal transformation is discussed in relation to the crystal packing structures of the VO^{IV} complexes.[13a] In contrast, [VO{(4-$C_nH_{2n+1}O)_x$salen}]ClO_4 with one (x = 1 and n = 3–16) and two (x = 2 and n = 3–10) long alkoxy chains in the 4-positions of the aromatic rings (Scheme 1) have been prepared in solutions in the presence of $HClO_4$ under aerobic conditions. The single point DFT molecular orbital calculations using the B3LYP method were carried out based on the crystal coordinates of [VO{(4-$C_3H_7O)_2$-salen}(MeOH)]ClO_4·0.5H_2O (**8**·MeOH·0.5H_2O) which shows a unique dimeric structure supported by electrostatic stacking and CH–π interactions between the aromatic rings and alkoxy chains in an octahedral environment. Moreover, in methanol solution, the effects of the alkoxy chain lengths on the ion-association state between [VO{(4-$C_nH_{2n+1}O)_x$-salen}]$^+$ and ClO_4^- were investigated by the conductometric method and the ion-association state in methanol solution is discussed along with that of the solid-state. It is of fundamental interest to elucidate the physico-chemical properties such as the ion-association state in solution.

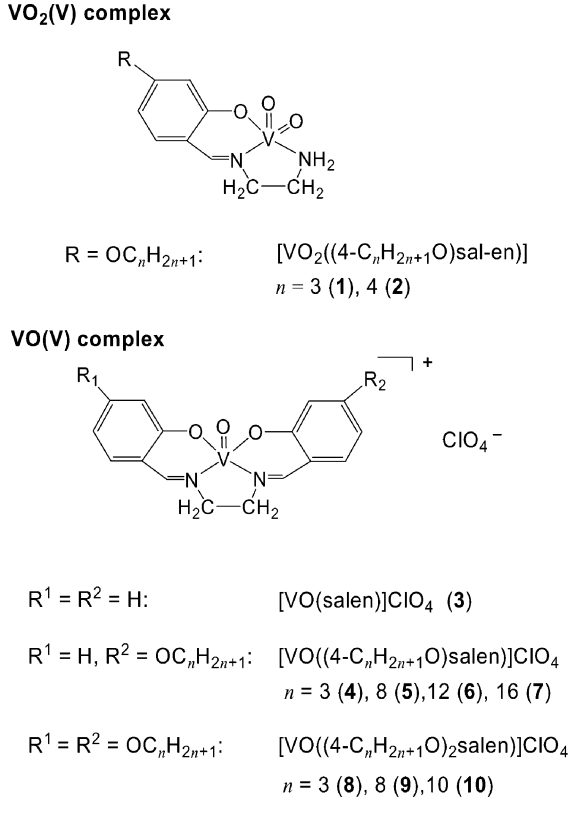

Scheme 1.

Results and Discussion

Synthesis and Characterisation of Complexes 1–10

Complexes **1** and **2** were obtained by the crystal-to-crystal transformations of the crystals of the VO^{IV} complexes, [VO{(4-$C_nH_{2n+1}O)_2$salen}] (n = 3, 4), coexisting with solutions under aerobic conditions. When the crystals of the VO^{IV} complexes were completely dissolved, the green VO^{IV} complexes did not change into the yellow VO_2^V complexes. As shown in Table 1, the IR spectra of **1** and **2** show strong bands at 931 cm^{-1} and 838 cm^{-1} for **1** and 939 cm^{-1} and 848 cm^{-1} for **2** which can be assigned to asymmetric and symmetric vibrations of the *cis*-VO_2 groups, respectively, in agreement with the case of the reported complexes with *cis*-VO_2 groups.[14] The EPR spectra for **1** and **2** were silent, indicating that **1** and **2** are changed to the +V oxidation state from the +IV oxidation state. The structures of **1** and **2** were determined by X-ray crystallography as described in the following section.

Table 1. Absorption maxima (br. = broad) and $E_{1/2}$ values in DMF and the characteristic IR bands for complexes **1**–**10**.

	n	λ_1/nm	logε	Abs. in DMF $\lambda_{2(br.)}$/nm	logε	CV in DMF $E_{1/2}$ vs. Ag/Ag^+	IR (V = O) cm^{-1}
1	3	298	4.408	360	4.044	–	931, 838
2	4	297	4.229	361	3.898	–	939, 848
3	0	284	4.275	570	3.104	–0.076	981
4	3	293	4.348	581	3.214	–0.073	981
5	8	294	4.353	582	3.210	–0.072	983
6	12	294	4.378	582	3.211	–0.072	983
7	16	294	4.328	582	3.217	–0.072	983
8	3	301	4.451	588	3.251	–0.050	988
9	8	301	4.382	589	3.227	–0.047	988
10	10	302	4.382	589	3.227	–0.047	988

In contrast, the addition of an $HClO_4$ solution to two series with one and two alkoxy chains in the 4-positions, [VO{(4-$C_nH_{2n+1}O)_x$salen}] (x = 1, 2), under aerobic conditions immediately afforded the corresponding blue VO^V perchlorate complexes [VO{(4-$C_nH_{2n+1}O)_x$salen}]ClO_4 [x =

1 (**4**–**7**), x = 2 (**8**–**10**)] without transformation of the salen moieties.[9b] The electronic absorption spectra of **4**–**10** exhibited broad absorption bands at 581–582 nm and 588–589 nm with the one (**4**–**7**) and two alkoxy chain substituents (**8**–**10**) on the aromatic rings, respectively. These are shifted to longer wavelengths compared with a value of 570 nm for [VO(salen)]ClO_4 (**3**) in DMF. The IR data are slightly dependent on the alkoxy chain lengths of the aromatic rings. The values of the V=O stretching vibrations for **3**–**10** are between 981 and 988 cm^{-1} in which the intermolecular interactions between V=O groups does not occur. The presence of the linear chain interaction (···V=O···V=O···) usually shifts the absorption to lower energy (ca. 870 cm^{-1}). The $E_{1/2}$ values of –0.072 to –0.073 V vs. Ag/AgCl attributed to the VO^{V}/VO^{IV} redox couple for **4**–**7** are negatively shifted compared with those of –0.047 to –0.050 V for **8**–**10** in DMF. The EPR silence of **3**–**10** confirms the +V oxidation state as well as in **1** and **2**.

X-ray Crystal Structure Determination of Complexes 1 and 2

The ORTEP diagrams and crystal packings of **1** and **2** are given in parts a and b of Figures 1 and 2, respectively. The selected bond lengths and angles are listed in Tables 2 and 3. Complex **1** has a 1:1 stoichiometric ratio of a monomer and a bis(μ-oxido)-bridged dimer, [VO_2{(4-C_3H_7O)-sal-en}][(VO_2{(4-C_3H_7O)sal-en}$)_2$]·DMF, accompanying the change in the oxidation state from IV to V. The tetradentate Schiff base ligand transforms to a tridentate Schiff base ligand by releasing the one moiety of two aromatic moieties. The monomer in **1** shows a distorted trigonal-bipyramidal coordination geometry with the weak hydrogen-bonding interaction between the salen moiety and the proton of a neighbouring DMF molecule (O7···H41 2.55 Å). Tridentate Schiff base ligand is coordinated to the V2 atom meridionally by the amine nitrogen (V2–N3 2.140 Å), the imine nitrogen (V2–N4 2.121 Å) and the phenolate oxygen (V2–O7 1.910 Å) atoms. The imine nitrogen N4 atom and two oxido ligands with O5 (V=O) and O6 (V=O) atoms occupy the equatorial positions (V2–O5 1.620 Å and V2–O6 1.631 Å). The V^{V} atom sits almost in the least-triangular N4, O5, O6 plane. The V2–O5 and V2–O6 bonds show typical V=O distances but the O7–V2–N3 angle of 159.14° is far from 180°. The structure of the monomer in **1** is very similar to that of the VO_2(tridentate) complex of a distorted trigonal-bipyramidal structure.[15] The bis(μ-oxido)-bridged dimer in **1** has a crystallographic inversion centre with the pair of $VO_2{}^{V}$ atoms (V1···V1* 3.1120 Å) in an edge-sharing

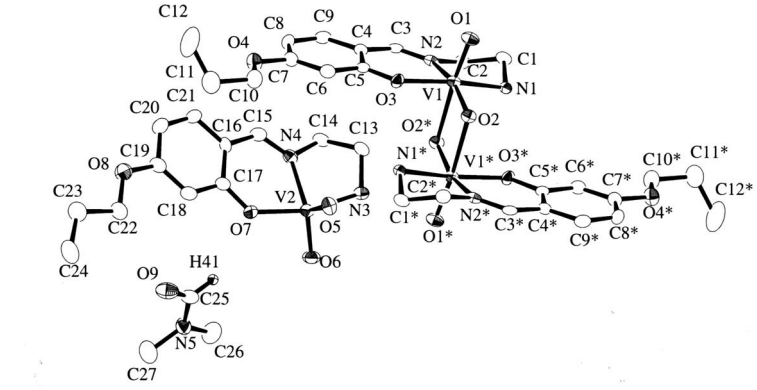

(a)

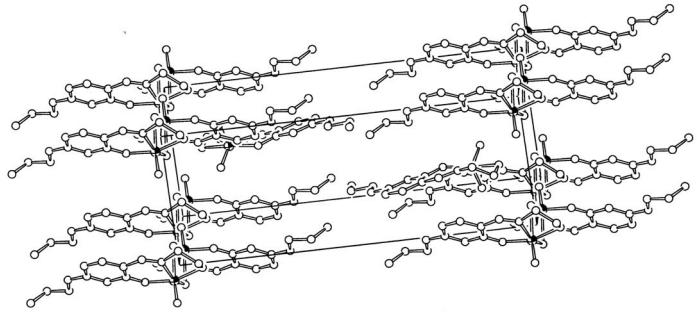

(b)

Figure 1. ORTEP plot (**a**) and crystal packing (**b**) of [VO_2{(4-C_3H_7O)sal-en}][(VO_2{(4-C_3H_7O)sal-en}$_2$)]·DMF (**1**). The hydrogen atom is omitted.

distorted octahedral geometry. The equatorial plane is occupied by the tridentate sal-en and oxido ligands (V1–N1 2.124 Å, V1–N2 2.165 Å, V1–O3 1.917 Å, and V1–O2 1.677 Å). The axial positions are coordinated by the terminal oxido ligand (V1–O1 1.625 Å) and the bridging oxido ligand with the weak interaction of the inversion related VO_2^+ group (V1–O2* 2.320 Å). The O1–V1–O2 angle of 105.04° is larger than 90° but the O1–V1–O2* angle of 171.21° is close to 180°. There are a few reports of structures similar to the bis(μ-oxido)-bridged dimer in **1**.[14] However, this is the first sample with the two different coordination geometries of which one is the distorted trigonal-bipyramidal monomer structure and the other is the bis(μ-oxido)-bridged dimer structure with the same Schiff base ligand in the crystal. The V=O distance for the bridging oxido ligand is much longer than those for the non-bridged oxido ligands in the monomer or dimer. The crystal structure of **1** clearly demonstrates that the van der Waals interactions between the monomer and dimer occur exclusively by the close contact between the sal-en moieties. The interactions which are shorter than 4 Å are C3···C13 3.544 Å, C4···C13 3.569 Å, C8···C15 3.406 Å and O4···C21 3.353 Å. In the light of the C11–H23···C_{arom} distances with

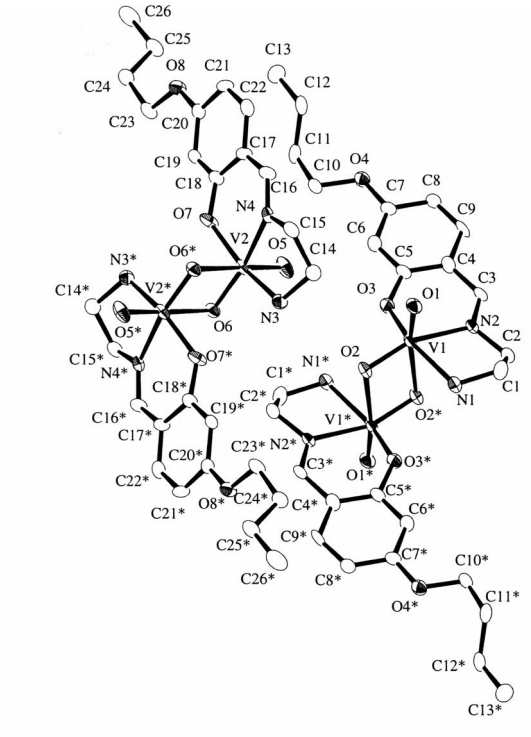

(a)

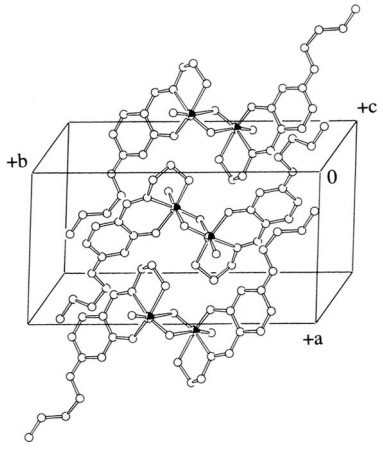

(b)

Figure 2. ORTEP plot (**a**) and crystal packing (**b**) of [(VO_2{(4-C_4H_9O)sal-en})$_2$] (**2**). The hydrogen atom is omitted.

Table 2. Selected bond lengths [Å] and angles [°] for complex **1**.

V1–O1	1.625(4)	V1–O2	1.677(2)
V1–O2*	2.320(3)	V1–O3	1.917(3)
V1–N1	2.124(3)	V1–N2	2.165(3)
V2–O5	1.620(3)	V2–O6	1.631(3)
V2–O7	1.910(3)	V2–N3	2.140(4)
V2–N4	2.121(4)	O3–C5	1.327(5)
O4–C7	1.364(6)	O4–C10	1.438(6)
O8–C19	1.354(6)	O8–C22	1.433(7)
O3–C5	1.327(5)	O7–C17	1.327(5)
O1–V1–O2	105.04(16)	O1–V1–O2*	171.21(14)
O1–V1–O3	102.36(17)	O1–V1–N1	90.97(17)
O1–V1–N2	97.58(16)	O2–V1–O2*	78.97(17)
O2–V1–O3	96.26(14)	O2–V1–N1	96.00(14)
O2*–V1–N1	80.76(15)	O2*–V1–N2	77.78(14)
O3–V1–N1	158.86(15)	O3–V1–N2	84.74(14)
N1–V1–N2	77.22(14)	O5–V2–O6	110.77(18)
O5–V2–O7	102.46(16)	O5–V2–N3	91.49(16)
O5–V2–N4	117.50(19)	O6–V2–O7	98.50(18)
O6–V2–N3	90.78(18)	O6–V2–N4	130.02(16)
O7–V2–N3	159.14(14)	O7–V2–N4	83.58(15)
N3–V2–N4	76.19(15)	V1–O2–V1*	101.03(14)

Table 3. Selected bond lengths [Å] and angles [°] for complex **2**.

V1–O1	1.613(4)	V1–O2	1.686(4)
V1–O2*	2.308(4)	V1–O3	1.923(4)
V1–N1	2.168(5)	V1–N2	2.188(5)
V2–O5	1.605(4)	V2–O6	1.699(4)
V2–O6*	2.264(4)	V2–O7	1.919(4)
V2–N3	2.156(5)	V2–N4	2.190(4)
O4–C7	1.368(7)	O3–C5	1.327(5)
O8–C20	1.358(7)	O4–C10	1.459(7)
O7–C18	1.333(7)	O8–C23	1.443(7)
O1–V1–O2	105.0(2)	O1–V1–O2*	169.6(2)
O1–V1–O3	100.9(2)	O1–V1–N1	91.4(2)
O1–V1–N2	96.8(2)	O2–V1–O2*	79.77(18)
O2–V1–O3	97.89(19)	O2–V1–N1	96.6(2)
O2–V1–N2	157.3(2)	O2*–V1–O3	87.49(17)
O2*–V1–N1	78.72(18)	O2*–V1–N2	77.71(17)
O3–V1–N1	157.9(2)	O3–V1–N2	84.10(19)
N1–V1–N2	76.20(19)	O5–V2–O6	105.4(2)
O5–V2–O6*	169.6(2)	O5–V2–O7	101.6(2)
O5–V2–N3	90.7(2)	O5–V2–N4	95.0(2)
O6–V2–O6*	79.95(17)	O6–V2–O7	98.9(2)
O6–V2–N3	96.6(2)	O6–V2–N4	158.6(2)
O6*–V2–O7	86.13(18)	O6*–V2–N3	76.69(18)
O6*–V2–N4	78.96(17)	O7–V2–N3	156.8(2)
O7–V2–N4	83.08(19)	N3–V2–N4	76.2(2)
V1–O2–V1*	100.2(2)		

H23···C16 3.859 Å, H23···C18 3.683 Å, H23···C19 3.080 Å, H23···C20 2.857 Å, H23···C21 3.268 Å, a CH–π interaction can be considered to have formed between the methylene proton of the alkoxy chains in the dimer and the aromatirc ring in the monomer. In addition, the amino protons in the dimer (N1–H1, N1–H2) and monomer (N3–H3, N3–H4) form the hydrogen bonds with the neighbouring oxygen atoms (H1···O5 2.053 Å, H2···O2 2.528 Å, H2···O3 2.385 Å, H2···O6 2.615 Å H3···O1 2.346 Å, H3···O2 2.703 Å, H4···O1 2.596 Å, H4···O2 2.577 Å, and H4···O3 2.734 Å).

In the case of n = 4 (Figure 2), **2** includes two bis(μ-oxido)-bridged dimers with slightly different V1···V1* and V2···V2* bond lengths of 3.0905 Å and 3.0584 Å, respectively, in the crystal (Table 4). The structure of **2** resembles that of the dimer in **1** which has an edge-sharing distorted octahedral geometry with similar bond lengths and angles. The CH–π interaction occurs exclusively between the dimers (C12–H21···C17 3.890 Å, H21···C18 4.072 Å, H21···C19 3.710 Å, H21···C20 3.139 Å, H21···C21 2.912 Å, H21···C22 3.320 Å). Furthermore, the oxygen atoms are hydrogen-bonded with the neighbouring amino group protons (N1–H37, N1–H38, N3–H35, N3–H36) with H37···O6 2.333 Å, H38···O2 2.498 Å, H38···O3 2.342 Å, H35···O2 2.590 Å, H36···O1 2.657 Å, H36···O6 2.488 Å, H36···O1 2.415 Å forming the hydrogen bonding network.

Table 4. Selected bond lengths [Å] and angles [°] for complex **8**·MeOH·0.5H_2O.

V1–O1	1.826(8)	V1–O2	1.829(8)
V1–O5	1.601(8)	V1–O6	2.298(8)
V1–N1	2.056(9)	V1–N2	2.066(10)
N1–C1	1.46(1)	N2–C2	1.45(1)
C7–O3	1.36(1)	C13–O4	1.35(1)
O1–V1–O2	106.6(3)	O1–V1–N1	85.9(4)
O2–V1–N2	86.2(4)	N1–V1–N2	76.7(4)
O1–V1–O5	102.8(4)	O2–V1–O5	99.2(4)
O5–V1–N1	97.6(4)	O5–V1–N2	90.6(4)
N1–V1–O6	80.2(3)	O5–V1–O6	173.2(4)
C7–O3–C17	18.7(9)	C14–O4–C20	115.1(6)
O3*–C13	3.77(2)	O3*–C14	3.59(1)
O4–C7*	3.71(2)	O4–C8*	3.77(2)
C6*–C15	3.55(2)	C7*–C14	3.69(2)
C8*–C20	3.59(2)		

Though the green crystal of the VO^{IV} complex with n = 6 changed to the yellow crystals, a single-crystal suitable for X-ray crystallography could not be obtained. Interestingly, the green crystals of the VO^{IV} complexes with longer alkoxy chains of $n \geq 8$ did not change to the yellow crystals of the $VO_2{}^V$ complexes. This crystal-to-crystal transformation depends significantly on the single-crystal structures of the square pyramidal VO^{IV} complexes with longer alkoxy chains.[13a] The VO^{IV} complexes of $n \geq 8$ form the bilayer structure assembled by only the VO^{IV} complex of which two alkoxy chains are arranged in the same direction. Thus, the neighbouring salen moiety penetrates into the space between two alkoxy chains with a dihedral angle of ca. 56° between the coordination planes. The stacking leads to a 1D structure layered to form a lamellar structure. The metal backbones interact by van der Waals contacts with each other in a lamellar structure. Thus, the molecules sit in the ridged crystal packings. In addition, the V=O groups as well as the planar salen moieties are not parallel with each other. Consequently, the VO^{IV} complexes with $n \geq 8$ could not transfer easily to form the $(VO)_2$ core of the bis(μ-oxido)-bridged dimer accompanying with the structural change from the square pyramidal to the octahedral geometry in addition to the transformation of the ligand and the oxidation state change from IV to V in the crystal. In contrast, the VO^{IV} complexes of n = 3, 4 and 6 form a dimeric structure with face-to-face van der Waals interactions.[13a] The dimeric complexes lead to a 1D stacking structure. Since the V=O groups as well as the planar salen moieties in the crystal are in parallel with each other, the oxygen atoms of the V=O groups are located near the neighbouring V atoms. Thus, the VO^{IV} complexes of n = 3, 4 and 6 may be able to transform to the $VO_2{}^V$ complex of the bis(μ-oxido)-bridged dimer without the larger structural changes in the crystals.

X-ray Crystal Structure and DFT Calculation of Complex 8·MeOH·0.5H_2O

The VO^V complex cation of **8**·MeOH·0.5H_2O, [VO{(4-$C_3H_5O)_2$salen}(MeOH)]$^+$ exhibits a distorted octahedral structure with the salen moiety forming the equatorial plane by means of the O1, O2, N1 and N2 atoms (V1–O1 1.826 Å, V1–O2 1.829 Å, V1–N1 2.056 Å, and V1–N2 2.066 Å), an oxido ligand and a methanol molecule occupying the axial sites (V1–O5 1.601 Å and V1–O6 2.298 Å), respectively (Table 4 and Figure 3). The V ion sits in the equatorial least square plane. The methanol oxygen atom weakly coordinates to the V atom and further interacts with the oxygen atom of the ClO_4^- counter anion through a hydrogen bond (O6···O7 2.76 Å and O6···H22 1.83 Å). In the crystal packing, the two complex cations form a dimeric structure without interaction between the two V=O groups (Figure 3). The VO^V and VO^{IV} complexes with 5- and 3-substituted salen derivatives, [VO(salen)](ClO_4),[9b] [VO(5-MeOsalen)(H_2O)](NO_3)H_2O[11] and [VO(3-EtOsalen)]-H_2O,[9d] show monomeric structures in the solid state and, consequently, the alkoxy chain group of the salen aromatic ring at the 4-postions should be responsible for the dimer formation. The octahedral monomers in **8**·MeOH·0.5H_2O are coupled with a crystallographically imposed centre of symmetry and the two V atoms are separated by 6.108 Å with the two O–V=O axes parallel each other. The dimer structure is supported exclusively by interactions between the aromatic rings of the ligands with the close contacts shorter than 4 Å (O3*···C13 3.77 Å, O3*···C14 3.59 Å, O4···C7* 3.71 Å, O4···C8* 3.77 Å, C6*···C15 3.55 Å, C7*···C14 3.69 Å, and C8*···C20 3.59 Å) (Figure 4). In addition, one of the methylene protons (H8 and H11) of the C17 and C20 atoms points directly to one of the phenyl rings. The quadruple CH–π interactions are present between the two complex cations (H8*···C12 2.95 Å,

H8*···C13 3.07 Å, H11···C4* 2.96 Å, H11···C8* 2.92 Å, and H11···C9* 2.79 Å). In general, the CH–π interaction has been regarded as one of the important attractive interactions in organic crystalline compounds although its individual energy is smaller than 1 kcal mol^{-1}.[16a]

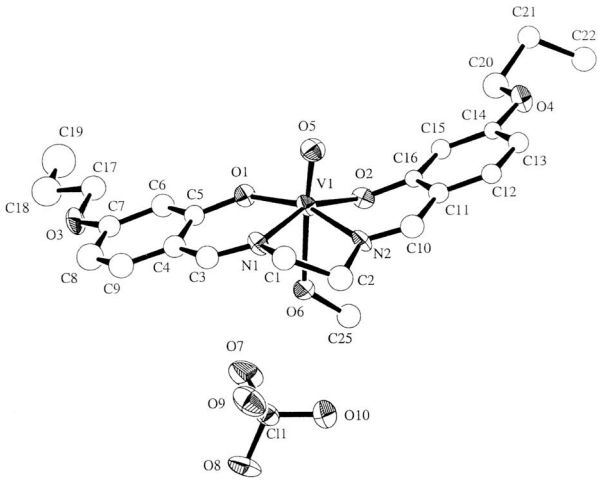

(a)

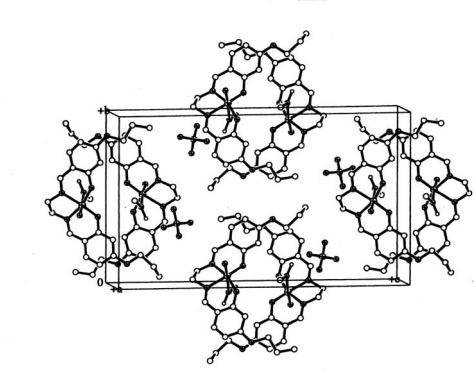

(b)

Figure 3. ORTEP plot (**a**) and crystal packing (**b**) of [VO{[4-$CH_3(CH_2)_2O]_2$salen}(MeOH)]ClO_4·0.5H_2O (**8**·MeOH·0.5H_2O). H_2O molecule and the hydrogen atom are omitted.

In the case of **1** and **2**, the crystal packings show polymeric structures resulting from the van der Waals forces, hydrogen bonding and CH–π interactions. However, $[VO\{(4\text{-}C_3H_5O)_2salen\}(MeOH)]^+$ in **8**·MeOH·0.5H_2O forms the dimeric structure by only the electrostatic and CH–π interactions. With regards to these interactions, single point DFT molecular orbital calculations using the B3LYP method were carried out on the dimeric and the monomeric structures of **8**·MeOH·0.5H_2O based on the crystal coordinates obtained in this work. The stabilisation energy for the dimer from the two separated monomers was calculated as 5.3 kcal mol^{-1} (0.23 eV) which is small but appreciable and indicates the presence of weak attractive interactions between the 4-substituted salen aromatic rings. Mulliken charge population for the dimer shows that the alkoxy-substituted phenyl carbons (C7* and C14) are positively charged (+0.34 and +0.36) and are electrostatically stacked with the negatively charged ether oxygen atoms [O3* (–0.31) and O4 (–0.26)] of the counterpart (Figure 4). From these structural and electronic features, the dimer structure of **8**·MeOH·0.5H_2O should be supported by both the electrostatic stacking and CH–π interactions between the alkoxy groups and the salen aromatic rings. A related dimer structure formed by both π-π stacking and CH–π interactions has been reported in the square planar Ni^{II} complex with the 5-butyl-substituted salen ligand[16b] but the present type of oxidovanadium dimer is, however, quite unusual.

Ion Association between $[VO\{(4\text{-}C_nH_{2n+1}O)_xsalen\}]^+$ (x = 0, 1, 2) and ClO_4^- in Methanol

Figure 5 shows the observed molar conductivities (Λ) of $[VO\{(4\text{-}C_nH_{2n+1}O)_xsalen\}]ClO_4$ as a function of the square root of the molar concentration (c). The conductivity data have been analysed using the Fuoss–Justice equation (see Exp. Sect.).[17] The values of Λ^∞, K_A and a obtained are listed in Table 5. To investigate the specific behaviour of the individual ions comprising these complex salts, it is neces-

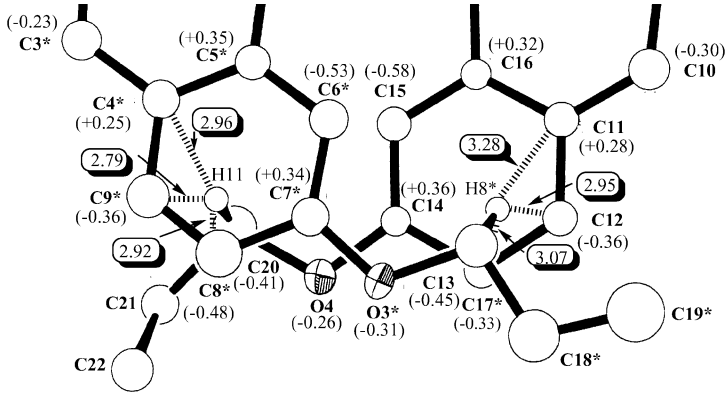

Figure 4. Mulliken charge population on the structures of the dimers (parts in which both electrostatic stacking and CH–π interactions are generated) and CH–π interaction distances less than 3.28 Å.

Table 5. Limiting molar conductivities of complex salts (Λ^∞), limiting molar conductivities of complex ions [VO{(4-$C_nH_{2n+1}O)_x$salen}]$^+$ (λ_+^∞), Walden products ($\lambda_+^\infty\eta$), Stokes radii (r_s), ion association constants (K_A) and the closest distances (a) between [VO{(4-$C_nH_{2n+1}O)_x$-salen}]$^+$ and ClO_4^- in MeOH.

Complex (x)	n	Λ^∞ S cm^2 mol^{-1}	λ_+^∞ S cm^2 mol^{-1}	$\lambda_+^\infty\eta$ S cm^2 mol^{-1} mPa s	r_s Å	K_A mol^{-1} dm^3	a Å
3 (0)	0	112.7 ± 0.6	41.7	22.7	3.61	60 ± 5	5.94
4 (1)	3	124.6 ± 0.3	53.6	29.2	2.81	88 ± 3	6.38
5 (1)	8	123.6 ± 0.6	52.6	28.7	2.86	91 ± 5	6.26
6 (1)	12	123.6 ± 0.9	52.6	28.7	2.86	84 ± 8	6.23
7 (1)	16	119.2 ± 0.7	48.2	26.3	3.12	88 ± 9	6.26
8 (2)	3	111.3 ± 1.2	40.3	22.0	3.73	71 ± 8	5.79
9 (2)	8	113.8 ± 1.1	42.8	23.3	3.52	85 ± 9	5.82
10 (2)	10	113.7 ± 0.9	42.7	23.3	3.52	95 ± 9	6.19

sary to divide the Λ^∞ values into the molar ionic conductivities, λ_+^∞ and λ_-^∞, where $\Lambda^\infty = \lambda_+^\infty + \lambda_-^\infty$. Using a value of 70.97 S cm^2 mol^{-1} for λ_-^∞ (ClO_4^-),[18] the values of λ_+^∞ for the complex cations were estimated and are listed in Table 5, together with those of the Walden product, $\lambda_+^\infty\eta$, and the Stokes radius, r_s [Å] = 82.0/($\lambda_+^\infty\eta$).

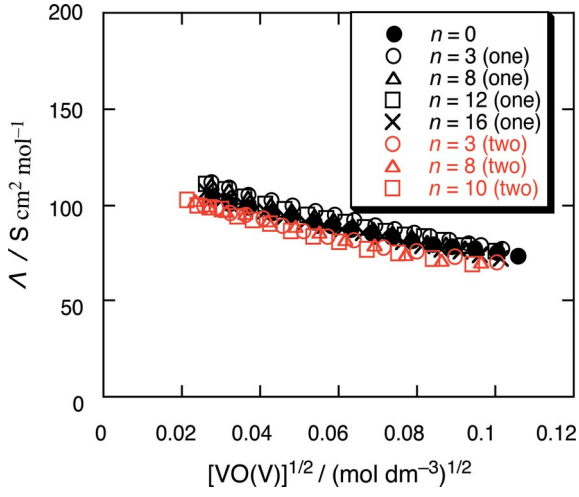

Figure 5. Molar conductances of [VO{(4-$C_nH_{2n+1}O)_x$salen}]ClO_4 (x = 0, x = 1, n = 3, 8, 12, 16 and x = 2, n = 3, 8, 10) in methanol solutions at 25 °C.

The λ_+^∞ values of the complex ions are 52.6–53.6 S cm^2 mol^{-1} for **4**–**6** with one alkoxy chain and 40.3–42.8 S cm^2 mol^{-1} for **8**–**10** with two alkoxy chains. These λ_+^∞ values are almost independent of the alkoxy chain length in each series. The λ_+^∞ value of the complex ion for **3**, [VO(salen)]ClO_4, without alkoxy chains is 41.7 S cm^2 mol^{-1} smaller than those for **4**–**7** with one alkoxy chain but close to those for **8**–**10** with two alkoxy chains. These tendencies are quite different from the case of the tetraalkylammonium ions for which λ_+^∞ values (S cm^2 mol^{-1}) decrease with an increase in the alkyl chain length, that is, Me_4N^+(68.7) > Et_4N^+(60.5) > Pr_4N^+(46.1) > Bu_4N^+(38.9) in methanol at 25 °C.[18,19] Although the complex ions of **4**–**7** have one alkoxy chain, their r_s values of 2.81, 2.86, 2.86 and 3.12 Å, respectively, are significantly smaller than 3.61 Å for [VO(salen)]$^+$ without alkoxy chains. This singular result can be interpreted for the following reason. The complex ion [VO(salen)]$^+$ may migrate with some rotational or rolling motion along the external electric field. When the complex ion has an alkoxy chain at its 4-position, the alkoxy chain may follow behind the salen moiety where the positive charge located at the central V atom responds to the external electric field, reducing the rotational and/or rolling motions of the salen moiety. This leads the plane of the planar salen ligand to become possibly parallel to the direction of the external electric field, reducing the friction between the salen moiety and the solvent. This reduction effect for the friction may be large enough to cause the r_s values of [VO{(4-$C_nH_{2n+1}O$)salen}]$^+$ to be smaller than that of [VO(salen)]$^+$ in spite of the alkoxy chain introducing the additional friction with the solvent. The similarities in the r_s values of the complex ions of **4**–**6** indicates that the increase of the friction between the alkoxy chain and the solvent with increasing the alkoxy chain length is cancelled out by the further reduction of the friction around the salen moiety based on the above-mentioned effect. The reason why the r_s values of 3.52–3.73 Å for the complex ions of **8**–**10** with two alkoxy chains are larger than those of 2.81–3.12 Å for **4**–**7** with one alkoxy chain may be the increase in friction due to the second alkoxy chain extending in a quite different direction from that of the first alkoxy chain, as shown in Figure 3 (a).

The values of the closest distance of approach, a, obtained for **3**–**10** are 5.8–6.4 Å. These values are not so different from each other. According to the ion-association theory of Yokoyama–Yamatera,[20] considering Coulombic interactions between ions, the values of K_A are expected to be 10.5 mol^{-1} dm^3 (a = 5.8 Å) and 9.4 mol^{-1} dm^3 (a = 6.4 Å) for the ion association between the univalent cation and anion in methanol at 25 °C. The observed K_A values for **3**–**10** are 60–95 mol^{-1} dm^3 which are significantly larger than the theoretical values, suggesting the presence of some extra interactions between [VO{(4-$C_nH_{2n+1}O)_x$salen}]$^+$ (x = 0, 1, 2) and ClO_4^-. The a values of 5.8–6.4 Å are close to the distance between the V atom and the centre of the perchlorate ion when one methanol molecule lies between them. The opposite approach of the perchlorate ion toward the V=O group may be improbable because the V=O oxygen atom is negatively charged and repulsive against the perchlorate ion. Therefore, the ion-association state most prob-

able is one in which the methanol molecule lies between the V atom and the perchlorate ion. Considering such an ion-association state, the following extra interactions may act between the ions. The first is the hydrogen bonding between the perchlorate ion and the methanol molecule which coordinates to the V atom as seen in their arrangement in the crystal structure of **8**·MeOH·0.5H_2O shown in Figure 3. The second is the ion–dipole interaction in addition to the ion–ion interaction because the complexes have not only electric charges but also some dipole moment roughly in the direction of the V=O bond axis. The values of K_A seem to be slightly increased by the introduction of the alkoxy groups from 60 $mol^{-1}\,dm^3$ for **3** to 71–95 $mol^{-1}\,dm^3$ for **4**–**10**. This suggests the strengthening of the hydrogen-bonding and/or the ion–dipole interaction due to some charge-distribution change within the complexes which might be introduced by the alkoxy groups.

Conclusions

Two series of Schiff base VO_2^V and VO^V complexes have been prepared from the Schiff base VO^{IV} complexes with 4-substituted long alkoxy chains on the aromatic rings. The crystal-to-crystal transformations from the VO^{IV} to the VO_2^V complexes occur when they have shorter alkoxy chains of n = 3, 4 and 6, and these accompany the transformation of the tetradentate ligand to the tridentate ligand. However, the crystal-to-crystal transformations did not occur for the VO^{IV} complexes with longer alkoxy chains of $n \geq 8$. The formation of the VO^V complexes is significantly influenced by the crystal packing structures of the VO^{IV} complexes. The complex salts of [VO{(4-$C_nH_{2n+1}O)_x$-salen}]ClO_4 with one (x = 1 and n = 3–16) and two (x = 2 and n = 3–10) alkoxy chains in the 4-positions were prepared in $HClO_4$/acetonitrile solution under aerobic conditions. The K_A values obtained from the conductivity measurements for methanol solutions of [VO{(4-$C_nH_{2n+1}O)_x$-salen}]ClO_4 are larger than those estimated by the ion-association theory, probably due to some extra interactions such as the hydrogen bonding between the complex ion and ClO_4^- through a methanol molecule. This ion-association state may be similar to that in the solid state.

Experimental Section

Reagents and Instrumentation: All chemicals and solvents of reagent grade were used without further purification. For the spectroscopic measurements, cyclic voltammetry and conductivity measurements, organic solvents of superfine reagent grade were dried with molecular sieves prior to use. The water content in methanol solution was confirmed to be 5–10 mmol dm^{-3} by the Karl Fischer method. The electronic absorption and the infrared spectra in KBr media were recorded on a Shimadzu UV-240 spectrophotometer and a JASCO FTIR-8900μ instrument, respectively. Cyclic voltammetry was performed using a Hokuto Denko HZ-1A apparatus. The measurements were carried out in DMF solution containing $n$$Bu_4NClO_4$ (0.1 mol dm^{-3}) as a supporting electrolyte. A three-electrode cell was used, including a glassy carbon working electrode, a platinum counter electrode and an Ag/Ag^+ reference electrode. Density functional calculations were performed using the B3LYP method with a lanl2dz basis set on a Silicon Graphic Octane Station with the Gaussian-94 program.

Conductivity Measurements: The electrical conductivity measurements were performed on methanol solutions of the complex salts, [VO{(4-$C_nH_{2n+1}O)_x$salen}]ClO_4 (x = 0, 1, 2), at 25.0 °C by using a Yanagimoto Conductimetric Apparatus MY-8. The observed molar conductivities (Λ) were analysed by using Equations (1), (2), (3), (4), and (5) to obtain the limiting molar conductivity, Λ^∞, the ion-association (ion-pair formation) constant, K_A, and the closest distance of approach of the ions, a.

$$\Lambda = \alpha\{\Lambda^\infty - S(\alpha c)^{1/2} + E(\alpha c)\log(\alpha c) + J_1(\alpha c) - J_2(\alpha c)^{3/2}\} \quad (1)$$

$$K_A = (1 - \alpha)/(\alpha^2 c y^2) \quad (2)$$

$$\log y = -A|z_+z_-|(\alpha c)^{1/2}/\{1 + Ba(\alpha c)^{1/2}\} \quad (3)$$

$$A = 1.8246 \times 10^6(\varepsilon_r T)^{-3/2} \quad (4)$$

$$B = 5.029 \times 10^9(\varepsilon_r T)^{-1/2} \quad (5)$$

α is the degree of dissociation (the fraction of free ions), y is the mean activity coefficient of free ions, ε_r is the relative dielectric constant of the solvent, z is the charge number of ions, T is the absolute temperature, and Equation (3) is the Debye–Hückel equation. For the conductivity, the Fuoss–Justice equation[17] [Equation (1)] was used. The values of ε_r and the viscosity coefficient η in the parameters (S, E, J_1, J_2) of Equation (1) were taken as 32.62 and 0.5445 mPa s, respectively, at 25.0 °C in methanol.[18] The values of Λ^∞, K_A, and a were determined to give a minimum of $\Sigma\{\Lambda(\text{calcd.}) - \Lambda(\text{obsd.})\}^2$ where Λ(calcd.) and Λ(obsd.) are the calculated and observed molar conductivities, respectively.

[VO_2{(4-C_3H_7O)sal-en}][(VO_2{(4-C_3H_7O)sal-en})$_2$]·DMF (1), [(VO_2-{(4-C_4H_9O)sal-en})$_2$] (2) and [VO(salen)]ClO_4 (3): [VO{(4-$C_nH_{2n+1}O)_2$-salen}] (n = 3, 4) and [VO(salen)]ClO_4 (**3**) were prepared following the procedure described in the literature.[13a,9b] The complexes of **1** (n = 3) and **2** (n = 4) were obtained from the slow transformation of the single crystals of [VO{(4-$C_nH_{2n+1}O)_2$salen}] coexisting with *N*,*N*-dimethylformamide (n = 3) and acetonitrile solutions (n = 4), respectively under aerobic conditions. This process took several months.

[VO{(4-$C_nH_{2n+1}O$)salen}]ClO_4 [n = 3 (4), 8 (5), 12 (6), 16 (7)]: Ethylenediamine (12.5 mmol) was added to a solution of 2,4-dihydroxybenzaldehyde (12.5 mmol) and 2-hydroxybenzaldehyde (12.5 mmol) in ethanol (40 mL) and the mixture was stirred at 60 °C for 30 min. The resultant (4-OH)salenH_2 (20 mmol) and $VOSO_4$·nH_2O (ca. 20 mmol) in the presence of CH_3COONa in ethanol (60 mL) was stirred at room temperature for 24 h. The precipitate was filtered off and washed with water, ethanol and diethyl ether. The reaction of [VO{(4-OH)salen}] (10 mmol) with BrC_nH_{2n+1} (n = 3, 8, 10, 12, 16) (40 mmol) in the presence of K_2CO_3 in DMF (150 mL) for several days gave the VO^{IV} complexes [VO{(4-$C_nH_{2n+1}O$)salen}] which were purified by passing through a silica-gel column, eluent was CH_2Cl_2/MeOH [20–25:1 (v/v)]. $C_{19}H_{20}N_2O_4V$ (n = 3) (391.31): calcd. C 58.31, H 5.15, N 7.16; found C 58.25, H 5.30, N 6.87. $C_{24}H_{30}N_2O_4V$ (n = 8) (461.45): calcd. C 63.86, H 6.70, N 6.21; found C 63.45, H 6.50, N 6.20. $C_{28}H_{38}N_2O_4V$·0.5H_2O (n = 12) (526.56): calcd. C 63.89, H 7.42, N 5.32; found C 63.91, H 7.23, N 5.57. $C_{32}H_{46}N_2O_4V$ (n = 16) (573.66): calcd. C 64.96, H 8.18, N 4.73; found C 64.86, H 8.08,

Table 6. Crystallographic and experimental data for complexes **1**, **2** and **8**·CH_3OH·$0.5H_2O$.

	1	**2**	**8**·CH_3OH·$0.5H_2O$
Empirical formula	$C_{27}H_{41}N_3O_{19}V_2$	$C_{13}H_{19}N_2O_4V$	$C_{23}H_{31}ClN_2O_{10.50}V$
Formula weight	681.53	318.25	589.9
Crystal colour, habit	yellow, plate	yellow, block	dark-blue, prismatic
Crystal dimensions [mm]	$0.20\times0.20\times0.05$	$0.35\times0.30\times0.20$	$0.48\times0.25\times0.15$
Crystal system	triclinic	triclinic	monoclinic
Space group	$P\bar{1}$ (no. 2)	$P\bar{1}$ (no. 2)	$P2_1/c$ (no. 14)
a [Å]	9.0396(5)	9.557(4)	7.263(7)
b [Å]	22.444(3)	17.662(8)	14.978(6)
c [Å]	8.0829(5)	8.451(2)	25.259(10)
α [°]	91.948(18)	91.82(3)	
β [°]	90.63(7)	92.07(4)	90.63(7)
γ [°]	86.186(15)	83.42(3)	
V [Å^3]	1544.2(2)	1415.5(10)	2747(2)
Z	2	4	4
D_{calc} [g cm^{-3}]	1.466	1.493	1.426
μ (Mo-K_α) [cm^{-1}]	6.637	7.147	5.15
$2\theta_{max}$ [°]	54.8	55	50
Observed reflections	10195 [$I > 2.00\sigma(I)$]	1600 [$I > 2.00\sigma(I)$]	2317 [$I > 3.00\sigma(I)$]
Variables	398	400	237
Temperature [°C]	–120	–120	–120
Residuals: R_1; wR_2[a]	0.0614; 0.1630	0.0929; 0.2088	0.096; 0.133

[a] $R_1 = \Sigma||F_o| - |F_c||/\Sigma|F_o|$. $wR_2 = \{[\Sigma w(F_o^2 - F_c^2)^2]/\Sigma[(wF_o^2)^2]\}^{1/2}$.

N 4.93. The obtained [VO{(4-$C_nH_{2n+1}O$)salen}] (n = 3, 8, 12, 16) (4.5 mmol) was dissolved in $HClO_4$/acetonitrile solution (7.6 mmol). The green solution immediately turned blue and was stirred for 1 h. After evaporation of the solvent, the precipitate was filtered and washed with water, ethanol and diethyl ether. The obtained precipitates were purified on Sephadex LH-20 (solvent: MeOH). These complexes were examined by elemental analysis and ESI-MS. $C_{19}H_{20}ClN_2O_8V\cdot3H_2O$ (n = 3) (544.81): calcd. C 41.89, H 4.81, N 5.14; found C 41.70, H 4.50, N 5.30. ESI-MS: 391.4. $C_{24}H_{30}ClN_2O_8V\cdot3H_2O$ (n = 8) (614.94): calcd. C 47.66, H 6.00, N 4.63; found C 47.52, H 5.80, N 4.50. ESI-MS: 461.4. $C_{28}H_{38}ClN_2O_8V\cdot H_2O$ (n = 12) (635.02): calcd. C 52.96, H 6.35, N 4.41; found C 52.68, H 6.25, N 4.60. ESI-MS: 517.6. $C_{32}H_{46}ClN_2O_8V\cdot H_2O$ (n = 16) (691.13): calcd. C 55.61, H 7.00, N 4.05; found C 55.82, H 7.12, N 4.25. ESI-MS: 574.2.

[VO{(4-$C_nH_{2n+1}O)_2$salen}]ClO_4 [n = 3(8), 8(9), 10(10)]: [VO{(4-$C_nH_{2n+1}O)_2$salen}] (n = 3, 8, 10) was prepared and the analyses were satisfactory as described elsewhere.[13a] [VO{(4-$C_nH_{2n+1}O)_2$-salen}]ClO_4 [n = 3(**8**), 8(**9**), 10(**10**)] as well as [VO((4-$C_nH_{2n+1}O$)-salen)]ClO_4 were prepared by the procedure as described above. Elemental analyses: $C_{22}H_{26}N_2O_9ClV\cdot0.5H_2O$ (n = 3) (557.85): calcd. C 47.37, H 4.88, N 5.02; found C 47.42, H 4.86, N 5.14. ESI-MS: 449.7. $C_{32}H_{46}ClN_2O_9V\cdot2H_2O$ (n = 8) (725.14): calcd. C 53.00, H 6.95, N 3.86; found C 52.89, H 6.68, N 3.98. ESI-MS:589.31. $C_{36}H_{54}ClN_2O_9V\cdot0.5H_2O$ (n = 10) (754.22): calcd. C 66.04, H 8.47, N 4.28; found C 66.00, H 8.34, N 4.28. ESI-MS: m/z = 645.78.

X-ray Crystallographic Analyses: Single crystals of complexes **1** and **2** suitable for X-ray crystallography were obtained from the slow transformation of the single crystals of [VO{(4-$C_nH_{2n+1}O)_2$salen}] present in *N*,*N*-dimethylformamide and acetonitrile solutions, respectively. Slow evaporation of a methanolic solution containing **8**·$0.5H_2O$ at room temperature yielded single crystal **8**·MeOH·$0.5H_2O$ suitable for X-ray crystallography. The X-ray diffraction data of **1** were collected at –120 °C on a Rigaku/MSC Mercury CCD diffractometer equipped with graphite-monochromated Mo-K_α radiation using a rotating-anode X-ray generator. The diffraction data of **2** and **8**·MeOH·$0.5H_2O$ were recorded on a Rigaku AFC8 and AFC7R instrument, respectively. The crystallographic data and experimental conditions are listed in Table 6. For **1** and **2**, a total of 1440 and 2160 oscillation images, covering the whole sphere of $2\theta < 54.8°$ and 55.0°, were collected with exposure rates of 240 and 128 s/° by the ω scan method ($-70 < \omega < 110°$ and $-62 < \omega < 118°$) and the crystal-to-detector (70×70 mm) distance was set to 60.27 and 59.51 mm, respectively. The data were processed using the Crystal Clear program[21a] and corrected for Lorentz polarisation and absorption effects. The structures were solved by direct methods (SIR92)[21,21b] and refined on F with the full-matrix least-squares techniques using the teXsan crystallographic software package.[21c] All non-hydrogen atoms were refined with anisotropic thermal parameters and the positions of the hydrogen atoms were calculated with d(C–H) = 0.95 Å and fixed in the refinement. All calculations were carried out on a Silicon Graphics O2 workstation running teXsan and on a Pentium®-based Personal Computer running the Crystal Structure package.[21,21d]

CCDC-630645 (for **1**), -630646 (for **2**) and -630647 (for **8**) contain the supplementary crystallographic data for this paper. These data can be obtained free of charge from The Cambridge Crystallographic Data Centre via www.ccdc.cam.ac.uk/data_request/cif.

Acknowledgments

This work was supported by a Nara Women's University Intramural Grant for Project Research.

[1] a) A. Butler, M. J. Clague, G. E. Meister, *Chem. Rev.* **1994**, *94*, 625–638; b) D. C. Crans, J. J. Smee, E. Gaidamauskas, L. Yang, *Chem. Rev.* **2004**, *104*, 849–902.
[2] T. Hirao, *Chem. Rev.* **1997**, *97*, 2707–2724.
[3] K. Kanamori, K. Nishida, N. Miyata, T. Shimoyama, K. Hata, C. Mihara, K. Okamoto, Y. Abe, S. Hayakawa, S. Matsugo, *Inorg. Chem.* **2004**, *43*, 7127–7140.
[4] a) J. L. Serrano, *Metallomesogens*, Wiley-VCH, Weinheim, **1996**; b) B. Donnio, D. W. Bruce, *in Structure and Bonding* (Ed.: D. M. P Mingos), vol. 95, Liquid Crystals II, Metallomesog-

ens, Springer, New York, **1999**; c) B. Donnio, D Guillon, R. Deschenaux, D. W. Bruce, *Metallomesogens* in *Comprehensive Coordination Chemistry II*, vol. 6 (Eds.: J. A. McCleverty, T. J. Meyer), Elsevier, Oxford, **2003**.

[5] a) T. Hegmann, F. Peidis, S. Diele, C. Tschierske, *Liq. Cryst.* **2000**, *27*, 1261–1265; b) M. Benouazzane, S. Coco, P. Espinet, J. Barbera, *J. Mater. Chem.* **2001**, *11*, 1740–1744; c) D. Pucci, G. Barberio, A. Crispini, O. Francescangeli, M. Ghedini, *Mol. Cryst. Liq. Cryst. Sect.* **2003**, *395*, 325–335; d) D. Pucci, G. Barberio, A. Crispini, O. Francescangeli, M. Ghedini, M. La Deda, *Eur. J. Inorg. Chem.* **2003**, 3649–3661; e) G. Barberio, A. Bellusci, A. Crispini, M. Ghedini, A. Golemme, P. Prus, D. Pucci, *Eur. J. Inorg. Chem.* **2005**, 181–188; f) D. Pucci, G. Barberio, A. Bellusci, A. Crispini, M. La Deda, M. Ghedini, E. I. Szerb, *Eur. J. Inorg. Chem.* **2005**, 2457–2463.

[6] a) X. H. Liu, M. N. Abser, D. W. Bruce, *J. Organomet. Chem.* **1998**, *551*, 271–280; b) L. Aiello, M. Ghhedini, M. La Deda, D. Pucci, O. Francesconi, *Eur. J. Inorg. Chem.* **1999**, 1367–1376; c) A. B. Blake, J. R. Chipperfield, W. Hussain, R. Paschke, E. Sinn, *Inorg. Chem.* **1995**, *34*, 1125–1129.

[7] a) H. Hoshino, H. Murakami, Y. Matsunaga, T. Inabe, Y. Maruyama, *Inorg. Chem.* **1990**, *29*, 1177–1181; b) R. Paschke, S. Diele, I. Letko, A. Wiegeleben, G. Pelzl, K. Grieser, M. Athanassopoulou, W. Haase, *Liq. Cryt.* **1995**, *18*, 451–456; c) R. Paschke, H. Zaschke, A. Maedicke, J. R. Chipperfield, A. B. Blake, P. G. Nelson, G. W. Gray, *Mol. Cryst. Liq. Cryst. Lett. Sect.* **1988**, *6*, 81–85; d) T. D. Shaffer, K. A. Sheth, *Mol. Cryst. Liq. Cryst. Sect.* **1989**, *172*, 27–39; e) R. Paschke, D. Balkow, U. Baumeister, H. Hartung, J. R. Chipperfield, A. B. Blake, P. G. Nelson, G. W. Gray, *Mol. Cryst. Liq. Cryst. Sect.* **1990**, *188*, 105–118.

[8] a) K. Ohta, Y. Morizumi, T. Fujimoto, I. Yamamoto, K. Miyamura, Y. Gohshi, *Mol. Cryst. Liq. Cryst. Sect.* **1992**, *214*, 161–169; b) R. Paschke, D. Balkow, E. Sinn, *Inorg. Chem.* **2002**, *41*, 1949–1953; c) M. Mathew, A. J. Carty, G. J. Palenik, *J. Am. Chem. Soc.* **1970**, *92*, 3197–3198; d) A. Serrette, P. J. Carroll, T. M. Swager, *J. Am. Chem. Soc.* **1992**, *114*, 1887; e) A. Serrette, T. M. Swager, *J. Am. Chem. Soc.* **1993**, *115*, 11656.

[9] a) P. E. Riley, V. L. Pecoraro, C. F. Carrano, J. A. Bonadies, K. N. Raymond, *Inorg. Chem.* **1986**, *25*, 154–160; b) J. A. Bonadies, W. M. Butler, V. L. Pecoraro, C. J. Carrano, *Inorg. Chem.* **1987**, *26*, 1218–1222; c) K. Nakajima, K. Kojima, S. Azuma, R. Kasahara, M. Tsuchimoto, Y. Kubozono, H. Maeda, S. Kashino, S. Ohba, Y. Yoshikawa, J. Fujita, *Bull. Chem. Soc. Jpn.* **1996**, *69*, 3207–3216; d) G. Hoshina, N. Tsuchimoto, S. Ohba, K. Nakajima, H. Uekusa, Y. Ohashi, M. Ishida, M. Kojima, *Inorg. Chem.* **1998**, *37*, 142–145.

[10] a) A. Hills, D. L. Hughes, G. J. Leigh, J. R. Sanders, *J. Chem. Soc. Chem. Commun.* **1991**, 827–829; b) A. Hills, D. L. Hughes, G. J. Leigh, J. R. Sanders, *J. Chem. Soc. Dalton Trans.* **1991**, 61–64; c) D. L. Hughes, U. Kleinkes, G. J. Leigh, M. Maiwald, J. R. Sanders, C. Sudbrake, *J. Chem. Soc. Dalton Trans.* **1994**, 2457–2466; d) N. F. Choudhary, N. G. Connelly, P. B. Hitchcock, G. J. Leigh, *J. Chem. Soc. Dalton Trans.* **1999**, 4437–4446.

[11] M. Tsuchimoto, E. Yasuda, S. Ohba, *Chem. Lett.* **2000**, *29*, 562–563.

[12] a) A. Cotton, G. Wilkinson, *Advanced Inorganic Chemistry*, 4th ed., Interscience, New York, **1987**.

[13] a) Y. Abe, K. Nakabayashi, N. Matsukawa, H. Takashima, M. Iida, T. Tanase, M. Sugibayashi, H. Mukai, K. Ohta, *Inorg. Chim. Acta* **2006**, *359*, 3934–3946; b) Y. Abe, H. Akao, Y. Yoshida, H. Takashima, T. Tanase, H. Mukai, K. Ohta, *Inorg. Chim. Acta* **2006**, *359*, 3147–3155; c) Y. Abe, N. Nakazima, T. Tanase, S. Katano, H. Mukai, K. Ohta, *Mol. Cryst. Liq. Cryst. Sect.* **2007**, *466*, 129–147.

[14] a) X. Li, M. S. Lah, V. L. Pecoraro, *Inorg. Chem.* **1988**, *27*, 4657–4664; b) C. A. Root, J. D. Hoeschele, C. R. Cornman, J. W. Kampf, V. L. Pecoraro, *Inorg. Chem.* **1993**, *32*, 3855–3861; c) A. C. Gonzalez-Baró, E. E. Castellano, O. E. Piro, B. S. Parajón-Costa, *Polyhedron* **2005**, *24*, 49–55.

[15] a) L. M. Mokry, C. J. Carrano, *Inorg. Chem.* **1993**, *32*, 6119–6121; b) G. Asgedom, A. Sreedhara, J. Kivikoski, E. Kolehmainen, C. P. Rao, *J. Chem. Soc. Dalton Trans.* **1996**, 93–97; c) S. Pal, K. R. Radhika, S. Pal, *Z. Anorg. Allg. Chem.* **2001**, *627*, 1631–1637; d) E. Kwiatowski, G. Romanowski, W. Nowicki, M. Kwiatkowski, K. Suwiska, *Polyhedron* **2003**, *22*, 1009–1018; e) P. Plitt, H. Pritzkow, R. Krämer, *Dalton Trans.* **2004**, 2314–2320.

[16] a) M. Nishino, M. Hirota, Y. Umezawa, *The CH/π Interaction. Evidence, Nature and Consequences*, Wiley-VCH, New York, **1998**; b) K. Miyamura, A. Mihara, T. Fujii, Y. Gohshi, Y. Ishii, *J. Am. Chem. Soc.* **1995**, *117*, 2377–2378.

[17] a) E. Renard, J.-C. Justice, *J. Solution Chem.* **1974**, *3*, 633–647; b) J. Quint, A. Viallard, *J. Solution Chem.* **1978**, *7*, 533–548; c) H. Yokoyama, T. Ohta, *Bull. Chem. Soc. Jpn.* **1988**, *61*, 3073–3076.

[18] R. L. Kay, C. Zawoyski, D. F. Evans, *J. Phys. Chem.* **1965**, *69*, 4208–4215.

[19] J. Barthel, M. Krell, L. Iberl, F. Feuerlein, *J. Electroanal. Chem.* **1986**, *214*, 485–505.

[20] H. Yokoyama, H. Yamatera, *Bull. Chem. Soc. Jpn.* **1975**, *48*, 1770–1776.

[21] a) *Crystal Clear 1.3.5*: Operating software for the CCD detector system. Rigaku and Molecular Structure Corp. **2003**; b) A. Altomare, M. C. Burla, M. Camalli, M. Cascarano, C. Giacovazzo, A. Guagliardi, G. Polidori, *J. Appl. Crystallogr.* **1994**, *27*, 435–438; c) *TEXSAN*: Crystal Structure Analysis Package, Molecular Structure Corp. **1999**; d) Crystal Structure 3.6: Crystal Structure Analysis Package, Rigaku and Molecular Structure Corp., **2003**.

Received: October 16, 2007
Published Online: March 28, 2008

